

Algorithms and analytical solutions for rapidly approximating long-term dispersion from line and area sources

Steven R.H. Barrett*, Rex E. Britter

University of Cambridge, Department of Engineering, Trumpington Street, Cambridge CB2 1PZ, UK

ARTICLE INFO

Article history:

Received 15 July 2008

Received in revised form

11 March 2009

Accepted 13 March 2009

Keywords:

Dispersion modelling

Long-term average concentrations

Area sources

Line sources

ABSTRACT

Predicting long-term mean pollutant concentrations in the vicinity of airports, roads and other industrial sources are frequently of concern in regulatory and public health contexts. Many emissions are represented geometrically as ground-level line or area sources. Well developed modelling tools such as AERMOD and ADMS are able to model dispersion from finite (i.e. non-point) sources with considerable accuracy, drawing upon an up-to-date understanding of boundary layer behaviour. Due to mathematical difficulties associated with line and area sources, computationally expensive numerical integration schemes have been developed. For example, some models decompose area sources into a large number of line sources orthogonal to the mean wind direction, for which an analytical (Gaussian) solution exists. Models also employ a time-series approach, which involves computing mean pollutant concentrations for every hour over one or more years of meteorological data. This can give rise to computer runtimes of several days for assessment of a site. While this may be acceptable for assessment of a single industrial complex, airport, etc., this level of computational cost precludes national or international policy assessments at the level of detail available with dispersion modelling. In this paper, we extend previous work [S.R.H. Barrett, R.E. Britter, 2008. Development of algorithms and approximations for rapid operational air quality modelling. *Atmospheric Environment* 42 (2008) 8105–8111] to line and area sources. We introduce approximations which allow for the development of new analytical solutions for long-term mean dispersion from line and area sources, based on hypergeometric functions. We describe how these solutions can be parameterized from a single point source run from an existing advanced dispersion model, thereby accounting for all processes modelled in the more costly algorithms. The parameterization method combined with the analytical solutions for long-term mean dispersion are shown to produce results several orders of magnitude more efficiently with a loss of accuracy small compared to the absolute accuracy of advanced dispersion models near sources. The method can be readily incorporated into existing dispersion models, and may allow for additional computation time to be expended on modelling dispersion processes more accurately in future, rather than on accounting for source geometry.

© 2009 Elsevier Ltd. All rights reserved.

1. Introduction

Operational dispersion modelling on the local scale (~ 10 km) is frequently performed to analyze compliance with air quality regulations and/or to assess potential public health impacts of new developments or policies. A recent example is the UK Department for Transport (2006) analysis of Heathrow Airport, UK. Violation of the planned annual average NO₂ ambient air quality standard was a major concern at Heathrow, but – partially on account of dispersion

modelling results – the UK Government has since proposed expansion of Heathrow (UK Department for Transport, 2007).

There are a number of widely used operational dispersion models applied in a regulatory or policy analysis context. Examples include ADMS (CERC, 2004; Carruthers et al., 1994, 1999; McHugh et al., 2001); AERMOD (Cimorelli et al., 2004); and LASAT (Janicke Consulting, 2009)¹. Other models are listed, for example, on the US Environmental Protection Agency website.²

* Corresponding author.

E-mail addresses: steven.barrett@eng.cam.ac.uk (S.R.H. Barrett), rb11@cam.ac.uk (R.E. Britter).

¹ Also see <http://www.austal2000.de> for information on the related AUSTAL2000 model.

² EPA Dispersion Modeling website. URL: <http://www.epa.gov/scram001/dispersionindex.htm>.

ADMS and AERMOD can be described as Gaussian plume models, while LASAT is a Lagrangian model. All have been widely applied and evaluated against experimental results demonstrating predictions of considerable accuracy (Carruthers et al., 1999; Hanna et al., 2001; McHugh et al., 2001; Perry et al., 2005; Hirtl and Baumann-Stanzer, 2007), but may require runtimes of hours to days. Runtime considerations are particularly acute when modelling long-term mean concentrations associated with arrays of area sources. For example, one-year simulations of Heathrow Airport, London, UK, using ADMS and AERMOD each took approximately one week in the UK Department for Transport (2006) Project for the Sustainable Development of Heathrow.

Estimating dispersion from point sources remains rapid in the sense that their simulation is not practically constrained by runtime concerns. However, due mathematical difficulties associated with accounting for line and area source geometry – particularly considering oblique wind directions – computationally expensive numerical integration is generally required. In the case of Gaussian line sources (i.e. a line source formed by integration of Gaussian point sources), an analytical solution is known for the case of a normal wind (Pasquill and Smith, 1983). No exact solution exists for oblique winds, but approximate solutions valid over a range of wind angles and receptor locations have been developed (Calder, 1973; Luhar and Patil, 1989; Esplin, 1995; Venkatram and Horst, 2006).³ These approximations can help in making long-term mean calculations more tractable, although switching between approximate solutions and numerical integration is necessary at certain wind directions. We are not aware of any similar mathematical approximations for oblique area sources or any approximations that directly yield long-term mean concentrations from line or area sources.

While direct application of advanced dispersion models such as AERMOD or ADMS may be tractable for detailed policy analyses at specific sites, this is not so for large-scale national or international policy assessments. For example, the authors are currently working on assessing local air quality impacts of airports globally, now and for future growth scenarios (Reynolds et al., 2007). This motivates our development of rapid methods of approximating long-term mean dispersion from line and area sources, as are appropriate for representing runways, terminal areas, etc. The purpose of this paper is to extend Barrett and Britter (2008), hereafter referred to as BB08, to develop a computationally efficient algorithm with supporting mathematical techniques for estimating long-term mean dispersion from line and area sources.

2. General approach

This section will describe our overall mathematical and algorithmic approach for approximating the long-term mean ground-level pollutant concentration, $\langle \chi(\mathbf{x}) \rangle$, due to a general source. We restrict ourselves to spatially constant emission rates, but allow for temporal correlation between emission rates and meteorology. Following sections will show how the general approach is applied to line and area sources, resulting in analytical solutions for long-term mean dispersion.

2.1. Notation

A spatial location is specified by the vector \mathbf{x} , while an element of a source is identified parametrically by a vector of variables \mathbf{t} . Typically \mathbf{t} would contain one member for a line source, or two for an area source, etc. The spatial location of an element of a source

identified by \mathbf{t} is denoted $\mathbf{x}(\mathbf{t})$. The plume direction (wind direction + 180°) is denoted by θ and the emission rate per unit length or area by q . We assume dispersion calculations account for some vector of meteorological variables, \mathbf{m} , which may include wind speed, friction velocity, Monin–Obukhov length, etc. We assume that a dispersion kernel $\chi_p(\dots)$ calculates the ground-level pollutant concentration due to a unit strength point source as a function of plume direction and meteorological variables. Evaluation of $\chi_p(\dots)$, in general, implies execution of an algorithm.

2.2. Conventional approaches

2.2.1. Time-series approach

Many current operational dispersion models calculate long-term mean concentrations by taking a time-series of meteorological observations, each averaged over a period ΔT , and evaluating the dispersion kernel for each period, i.e.

$$\langle \chi(\mathbf{x}) \rangle = \frac{1}{N} \sum_{i=1}^N \int q_i \chi_p(\theta_i, \mathbf{m}_i, \mathbf{x} - \mathbf{x}(\mathbf{t})) d\mathbf{t}, \quad (1)$$

where $i = 1, \dots, N$ index the time periods. Usually $\Delta T = 1$ h and N is a multiple of 8760 (i.e. one or more years). Note that the inner (generally numerical) integration is over spatial dimensions \mathbf{t} for each time-step.

2.2.2. Direct statistical approach

If the joint probability density function, $p(\theta, \mathbf{m}, q)$, can be computed, then the mean ground-level concentration due to a general source of constant spatial strength is given by the convolution over elements constituting the source

$$\langle \chi(\mathbf{x}) \rangle = \int \int \int p(\theta, \mathbf{m}, q) q \chi_p(\theta, \mathbf{m}, \mathbf{x} - \mathbf{x}(\mathbf{t})) dq d\mathbf{t} d\mathbf{m}. \quad (2)$$

Statistical approaches similar to this, along with the assumptions implicit in this type of dispersion modelling, have been discussed by Calder (1976) and Martin (1971). In this notation each nested integration would translate computationally into a loop structure (for-loop, etc.) with appropriate discretization of variables. Nested loops give the expected multiplicative increase in execution time. The notation of integration over a vector implies the number of nested loops associated with the length of the vector.

We note that a time-series approach is less efficient (or at best equally efficient) as compared to a statistical approach due to possible duplication of calculations. However, in some contexts – such as detailed analysis of specific pollution episodes associated with low wind conditions – time-series approaches remain the only practical method.

2.3. Application of rapid modelling techniques

2.3.1. The dispersion impact parameter

As a conceptual tool, we previously described a ‘dispersion impact parameter’ (BB08), defined as

$$I(\theta, \mathbf{m}) = \int p(\theta, \mathbf{m}, \tilde{q}) \tilde{q} d\tilde{q}, \quad (3)$$

with \tilde{q} normalized such that $\int p(\tilde{q}) \tilde{q} d\tilde{q} = 1$. Conceptually, the dispersion impact parameter quantifies the average impact a unit strength source has in each wind direction. Note that due to the definition of the dispersion impact parameter, all analyses that follow account for correlation between meteorological conditions and emissions. Given an emissions scaling \tilde{q} , using the pre-computed

³ Also see the line source modelling review by Nagendra and Khare (2002).

dispersion impact parameter reduces the number of nested loops by one:

$$\langle \chi(\mathbf{x}) \rangle = \int \int \int I(\theta, \mathbf{m}) \bar{q} \chi_p(\theta, \mathbf{m}, \mathbf{x} - \mathbf{x}(\mathbf{t})) dt d\theta d\mathbf{m}. \quad (4)$$

2.3.2. Receptor lateral dispersion averaging approximation

In BB08 we introduced the lateral dispersion averaging approximation (LDAA), which is similar to the sector averaged approach as applied in the ASPEN model (US EPA, 2000). This result is applicable when calculating long-term mean pollutant concentrations and allows a significant computational saving. A reference case described in BB08 demonstrated a reduction in computational cost by two orders of magnitude in exchange for a 2% error on an area-based metric. We will term this approximation ‘Receptor LDAA’ to distinguish it from a ‘Source LDAA’ that will be developed in this paper.

Receptor LDAA requires that a point source dispersion kernel can be multiplicatively decomposed into a vertical and lateral component, i.e.

$$\chi_p(\mathbf{m}, x, y) = \underbrace{\chi_v(\mathbf{m}, x)}_{\text{vertical}} \underbrace{\chi_l(\mathbf{m}, x, y)}_{\text{lateral}} \quad (5)$$

in conventional plume aligned coordinates for ground-level concentrations. The result of Receptor LDAA is that the need for integrating over wind directions is avoided provided that the point source dispersion kernel is replaced by the vertical dispersion kernel, divided by the distance from the source, which for general sources give

$$\langle \chi(\mathbf{x}) \rangle = \int \int I(\theta, \mathbf{m}) \bar{q} \frac{\chi_v(\mathbf{m}, |\mathbf{x} - \mathbf{x}(\mathbf{t})|)}{|\mathbf{x} - \mathbf{x}(\mathbf{t})|} dt d\mathbf{m}, \quad (6)$$

where θ is the plume angle corresponding to the vector $\mathbf{x} - \mathbf{x}(\mathbf{t})$ (BB08).

Lateral dispersion tends to smooth-out the angular changes in concentrations away from the source as compared to angular changes in the dispersion impact parameter. BB08 shows that this can be accounted for by convolving the dispersion impact parameter with the lateral dispersion kernel, i.e.

$$\bar{I}(\theta, \mathbf{m}) = I \chi_l = \int_{-\infty}^{\infty} I(\theta - \tilde{\theta}, \mathbf{m}) \chi_l(\tilde{\theta}, \mathbf{m}) d\tilde{\theta}, \quad (7)$$

where $\bar{I}(\theta, \mathbf{m})$ is a ‘smoothed dispersion impact parameter’. In this notation $\chi_l(\tilde{\theta}, \mathbf{m})$ is the value of χ_l at any (x, y) which makes an angle $\tilde{\theta}$ with the plume centre-line. For Source LDAA to be introduced presently, an analogous smoothing operation is required.

2.3.3. Source lateral dispersion averaging approximation

We now propose the approximation that, for each receptor, we can neglect changes in the dispersion impact parameter over angles extending from the source to the receptor. Thus for each receptor we propose evaluating $I(\theta, \mathbf{m})$ once at an effective angle, such as the angle from the receptor to the centre of the source. We term this ‘Source LDAA’.

This approach has utility where the functional form of $\chi_v(\dots)$ can be specified in such a way as to allow analytical evaluation of

$$\chi_a(\mathbf{m}, \mathbf{x}) = \int \frac{\chi_v(\mathbf{m}, |\mathbf{x} - \mathbf{x}(\mathbf{t})|)}{|\mathbf{x} - \mathbf{x}(\mathbf{t})|} dt. \quad (8)$$

In cases where this can be achieved, the nested computations required have again been further reduced so that

$$\langle \chi(\mathbf{x}) \rangle = \int I(\theta(\mathbf{x}), \mathbf{m}) \bar{q} \chi_a(\mathbf{m}, \mathbf{x}) d\mathbf{m}, \quad (9)$$

where $\theta(\mathbf{x})$ denotes an effective plume direction at location \mathbf{x} for the source of interest. Sections 3 and 4 will develop analytical solutions $\chi_a(\dots)$ for line and area sources, respectively, based on the functional form of $\chi_v(\dots)$ described in section 2.4.

Fig. 1 schematically contrasts the two lateral dispersion averaging approximations. Receptor LDAA derived in BB08 was concerned with assuming changes in $I(\theta, \mathbf{m})$ across the width of a plume at the receptor can be neglected. Source LDAA proposed here is conceptually the opposite – changes in $I(\theta, \mathbf{m})$ are neglected across the source from the receptor’s perspective.

As described in section 2.3.2, Receptor LDAA can be improved by smoothing the dispersion impact parameter with an averaging angle approximately equal to the plume angle. This smoothing operation accounts for lateral dispersion and was mathematically derived in BB08 for a point source. If we now consider general (e.g. area) sources, where Source LDAA is useful, an analogous smoothing operation is required to approximately capture the effect of the range of upwind angles influencing a particular receptor. The appropriate averaging algorithm will depend on the specific source geometry, but in general the dispersion impact parameter and vertical dispersion kernel should be smoothed over the range of upwind angles extending from a source to a particular receptor.

Comparing Eq. (9) to where we started – Eq. (2) – the expected number of dispersion algorithm executions could be reduced by a factor $O(n(q) \times n(\theta) \times n(t_1) \times n(t_2) \times \dots)$, where $n(\cdot)$ denotes the number of discretizations applied and t_1, t_2 , etc., are the members of \mathbf{t} . For example, the number of dispersion algorithm executions associated with an area source involving five discretized emission levels, 36 wind directions, and a 10×10 grid representing the source could be reduced by a factor of $5 \times 36 \times 10 \times 10$, i.e. about 99.99%. We expect operationally realized computational savings to be degraded from this as pre-processing and execution time for $\chi_a(\dots)$ have not been accounted for.

2.4. Functional form and parameterization

In order to make further progress analytically, it is necessary to specify the functional form of the vertical dispersion kernel for ground-level concentrations and to restrict our attention to specific source geometries. This will enable us to apply Source and Receptor LDAA to develop analytical approximations for long-term mean dispersion from ground-level line and area sources under idealized

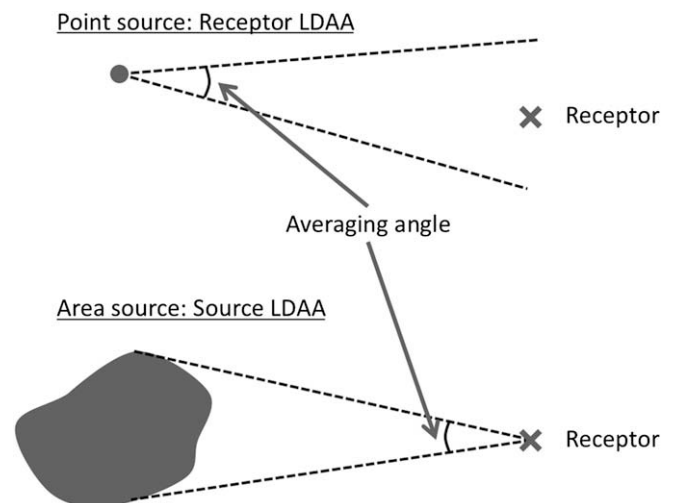


Fig. 1. Graphical depiction of Receptor and Source LDAA with angles over which the two-dimensional dispersion parameters are smoothed.

conditions. We then describe an operational approach to parameterize solutions based on a single run of an existing advanced dispersion model.

2.4.1. Functional form

For the current work we have selected the functional form

$$\chi_v(x) = \frac{A}{x^s} \tag{10}$$

as this proves mathematically tractable and considerable experimental evidence supports a power-law decay exponent $\sim 1/x^s$ for two-dimensional dispersion, e.g. Britter et al. (2003). Additionally, the K – theory theoretical framework supports a decay of the form $\sim 1/x^s$, with s constant (Pasquill and Smith, 1983). However, some formulations give rise to what can be interpreted as a decay exponent which varies slowly with distance, e.g. as in AERMOD (Cimorelli et al., 2004). Where this is the case, we consider the concentration decay to locally behave as $\sim 1/x^s$, where A and s take on locally accurate constant values. This introduces error to only the extent that A or s change over the upwind length of a source from the perspective of a specific receptor.

2.4.2. Operational parameterization method

While theoretical approaches for determining I , A and s directly may be developed (e.g. from K – theory), for the purposes of the current paper we describe an operational approach which makes use of existing advanced dispersion models. This method requires one additional assumption: That long-term average concentrations from a point source can locally be approximated by Eq. (10).

The method requires a single dispersion model run for one or more years of meteorological data, applied to a single ground-level point source in a polar coordinate system to produce an $M \times N$ matrix of concentration estimates \mathbf{C} , where there are $i = 1, \dots, M$ plume directions, \mathbf{T} , and there are $j = 1, \dots, N$ receptor distances from the point source, \mathbf{R} . The dispersion model run would be for an average source strength Q_p , and have the desired temporal emissions profile.

If a time-series dispersion model is used, e.g. AERMOD, then $I(\theta, \mathbf{m})$ is not required as its effects are incorporated into \mathbf{C} . We thus only need parameterize A and s . This is done at discrete locations in matrices \mathbf{A} and \mathbf{s} , which are of size $M \times (N - 1)$. A and s are assumed locally constant. It follows from the chosen functional form [i.e. Eq. (10)], they take on values

$$s_{ij} = \frac{\log(C_{ij}/C_{i,j+1})}{\log(R_{j+1}/R_j)} - 1 \Rightarrow A_{ij} = \frac{C_{ij}}{Q_p R_j^{s_{ij}+1}}$$

The $- 1$ arises to recover two-dimensional decay from a three-dimensional model output. Given a mean pollutant emission rate Q (recalling that correlation between meteorology and emissions are incorporated into the parameterization run), the mean pollutant concentration is given by $\langle \chi \rangle = Q\chi_a/Q_p$, with χ_a as per Eq. (8), A and s interpolated from \mathbf{A} and \mathbf{s} after pre-smoothing over upwind angles which influence a particular receptor.

We emphasize here the key computational saving: by developing an analytical solution for line and area sources under isotropic meteorological conditions, and applying the operational parameterization, we reduce the computational requirements from lengthy nested numerical integration and repeated calculation to evaluation of an analytical equation and a single (rapid) point source dispersion calculation.

3. Line source modelling

We now apply the general approach of section 2 to the case of a line source. We begin by applying Receptor LDAA to reduce the

number of nested numerical integrations required, then Source LDAA to allow development of an analytical approximation of long-term mean dispersion.

3.1. Direct statistical approach

Consider the line source of width w at an angle γ to the Y -axis shown in Fig. 2. Geometric considerations give the annual average concentration from application Eq. (2) as

$$\langle \chi(X, Y) \rangle = \int \int \int_0^{w \cos \gamma} \int_0^{\tilde{Y} \tan \gamma} (q/\cos \gamma)(\theta, \mathbf{m}, q) \times \chi_p(\theta, \mathbf{m}, X - \tilde{Y} \tan \gamma, Y - \tilde{Y}) d\tilde{Y} dq d\mathbf{m} d\theta, \tag{11}$$

where χ_p is the dispersion kernel for a point source of unit strength and $q/\cos \gamma$ is the source strength per unit length, q , projected onto the Y -axis over which the integration is performed.

3.2. Application of Receptor LDAA

We now apply Receptor LDAA to simplify the calculation of long-term mean dispersion from line sources. Given a vertical dispersion kernel χ_v and a dispersion impact parameter $I(\theta, \mathbf{m})$, application of Receptor LDAA gives

$$\langle \chi(X, Y) \rangle = \frac{\bar{q}}{\cos \gamma} \int_0^{w \cos \gamma} \int_0^{\tilde{Y} \tan \gamma} I(\theta, \mathbf{m}) \frac{\chi_v(\mathbf{m}, x)}{x} d\tilde{Y} d\mathbf{m}, \tag{12}$$

where $x = (X_I^2 + Y_I^2)^{1/2}$, $X_I = X - \tilde{Y} \tan \gamma$, $Y_I = Y - \tilde{Y}$,

$$\theta = \begin{cases} \theta_I, & X_I \geq 0 \text{ and } Y_I \geq 0, \\ \theta_I + \pi, & Y_I < 0, \\ \theta_I + 2\pi, & X_I < 0 \text{ and } Y_I \geq 0, \end{cases} \tag{13}$$

and $\theta_I = \tan^{-1}(X_I/Y_I)$. This approach is necessary as $\tan^{-1}(\cdot)$ does not retain information about quadrants. For example, $\tan^{-1}(-/-) = \tan^{-1}(+/+)$, which would give an angle for quadrant I when quadrant III was intended. Note that the $x - y$ frame translates and rotates along the line source as the integration proceeds, with the x pointing towards (X, Y) . This is on account of the implication of Receptor LDAA

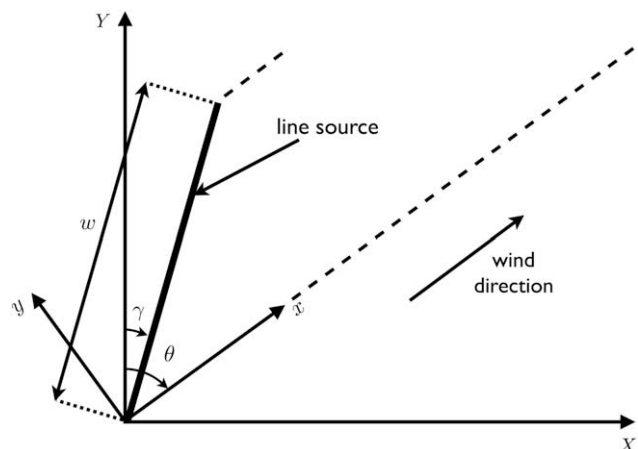


Fig. 2. Schematic of a line source at angle γ and width w .

that only elements of sources directly upwind need to be considered for calculating long-term mean dispersion.

3.3. Application of Source LDAA

Here we determine the analytical solution for long-term dispersion from a finite line source in isotropic meteorological conditions. The parameterization method described in section 2.4 will allow us to relax this assumption upon application.

The geometry of a (spatially) constant strength line source is shown in Fig. 2. Invoking the approximation of sections 2.3.3 and 2.4, the annual average concentration is given by evaluation of Eq. (9), where χ_a is given by Eq. (8) and χ_v is given by Eq. (10), i.e.

$$\chi_a(X, Y) = \frac{A}{\cos \gamma} \int_0^{w \cos \gamma} \left[(X - \tilde{Y} \tan \gamma)^2 + (Y - \tilde{Y})^2 \right]^{-\frac{s+1}{2}} d\tilde{Y}, \quad (14)$$

where the power of a half arises from determining the length $|\mathbf{x} - \mathbf{x}(\mathbf{t})|$.

The integral [Eq. (14)] can be expressed in closed form. We first consider the limiting case of $s = 1$. Integration and algebraic rearrangement results in

$$\chi_a(X, Y)|_{s=1} = \frac{A \left\{ \tan^{-1} \left[\frac{X \sin \gamma + Y \cos \gamma}{X \cos \gamma - Y \sin \gamma} \right] - \tan^{-1} \left[\frac{X \sin \gamma + Y \cos \gamma - w}{X \cos \gamma - Y \sin \gamma} \right] \right\}}{X \cos \gamma - Y \sin \gamma}. \quad (15)$$

This corresponds to a three-dimensional version of the neutral stability uniform boundary layer solution found by Calder (1952), which was used to simply demonstrate application of Receptor LDAA in BB08.

We now examine the more realistic case of $s < 1$ (with $s = 1$ integration of χ_v to represent an area source results in infinite ground-level concentrations). To simplify notation we set $\gamma = 0$ and rewrite Eq. (14) as

$$\chi_a(X, Y) = A \int_0^w \left\{ X^2 \left[1 + \left(\tilde{Y}/X - Y/X \right)^2 \right] \right\}^{-\frac{s+1}{2}} d\tilde{Y}.$$

Using the change of variable $t = \tilde{Y}/X - Y/X \Rightarrow dt = d(\tilde{Y}/X)$ results in

$$\chi_a(X, Y) = \frac{A}{|X|^s} \int_0^{w'} \left[1 + t^2 \right]^{-\frac{s+1}{2}} dt,$$

where $w' = (w - Y)/X$. From this we find that

$$\chi_a(X, Y) = \frac{A}{|X|^{s+1}} \left[Y {}_2F_1 \left(\frac{1}{2}, \frac{s+1}{2}; \frac{3}{2}; -\frac{Y^2}{X^2} \right) - (Y - w) {}_2F_1 \left(\frac{1}{2}, \frac{s+1}{2}; \frac{3}{2}; -\frac{(Y - w)^2}{X^2} \right) \right], \quad (16)$$

where ${}_2F_1(\dots)$ is Gauss's hypergeometric function (Abramowitz and Stegun, 1964). This solution can, of course, be rotated and translated straightforwardly. Note the property of the hypergeometric function

$${}_2F_1 \left(\frac{1}{2}, 1; \frac{3}{2}; -t^2 \right) = t^{-1} \tan^{-1} t$$

(Abramowitz and Stegun, 1964) relates Eq. (16) to the uniform boundary layer case of Eq. (15).

Eq. (16) is an analytical solution for long-term mean dispersion from a line source. To the extent that vertical dispersion is

represented by a power-law decay, it is exact in cases where the $I(\theta, \mathbf{m})$ is isotropic (i.e. constant in θ), or can be approximately applied when $I(\theta, \mathbf{m})$ varies angularly using Source LDAA. In the form presented, it can be directly applied in all quadrants.

While finite sources are of practical interest, infinite sources are of some theoretical interest. The solution for long-term mean dispersion from an infinite line source, assuming isotropic meteorological conditions, can be analytically expressed by evaluation of

$$\chi_a(X, Y) = \frac{A}{|X|^s} \int_{-\infty}^{\infty} \left[1 + t^2 \right]^{-\frac{s+1}{2}} dt,$$

which yields

$$\chi_a(X) = \frac{A}{|X|^s} \frac{\Gamma\left(\frac{s}{2}\right) \sqrt{\pi}}{\Gamma\left(\frac{s+1}{2}\right)}, \quad (17)$$

where $\Gamma(\cdot)$ is the Gamma function (Abramowitz and Stegun, 1964). For example, if $s = 0.8$ (a typical value), then $\chi_a(X) = 3.68A|X|^{-0.8}$. This result agrees with our intuition that the $\sim X^{-s}$ law transfers from two-dimensional dispersion to three-dimension dispersal for an infinite source, except with a correction factor that accounts for a component of off-normal winds contributing to the overall mean concentration.

4. Area source modelling

We now apply the general approach of section 2 to the case of area sources. We begin by applying Receptor LDAA to reduce the number of nested numerical integrations required. This is described for arbitrary area sources. Source LDAA will then allow development of an analytical approximation of long-term mean dispersion from rectangular area sources, drawing upon results of section 3.

4.1. Direct statistical approach

Given some pollutant emission rate q the annual mean pollutant concentration is given by the convolution of Eq. (2) over X and Y as in

$$\langle \chi(X, Y) \rangle = \int \int \int \int p(\theta, \mathbf{m}, q) \times q \chi_p(\theta, \mathbf{m}, X - \tilde{X}, Y - \tilde{Y}) dq d\tilde{X} d\tilde{Y} d\theta d\mathbf{m}. \quad (18)$$

4.2. Application of Receptor LDAA to arbitrary area sources

We now apply Receptor LDAA to simplify the calculation of long-term mean dispersion from arbitrary area sources. Fig. 3 shows an example area source, and defines r as the upwind distance to the leading edge of the area source, and l as the upwind length of the area source. Both r and l are functions of receptor location and plume direction. These variables are of relevance as Receptor LDAA implies that, for calculating long-term mean concentrations, only source elements directly upwind need to be considered when integrating over the dispersion impact parameter.

We change to polar coordinates (θ, x) , where θ is the plume direction and x is the distance from the upwind leading edge of the area source to a source element of area $\delta x \times (r - x) \delta \theta$. The annual average concentration due to an area source is thus given by

$$\langle \chi(X, Y) \rangle = \int \int \int I(\theta, \mathbf{m}) \underbrace{\frac{\chi_v(r-x, \mathbf{m})}{r-x}}_{\text{Receptor LDAA}} \times \underbrace{\bar{q} \times (r-x)}_{\text{Emission rate}} dx d\theta d\mathbf{m}. \quad (19)$$

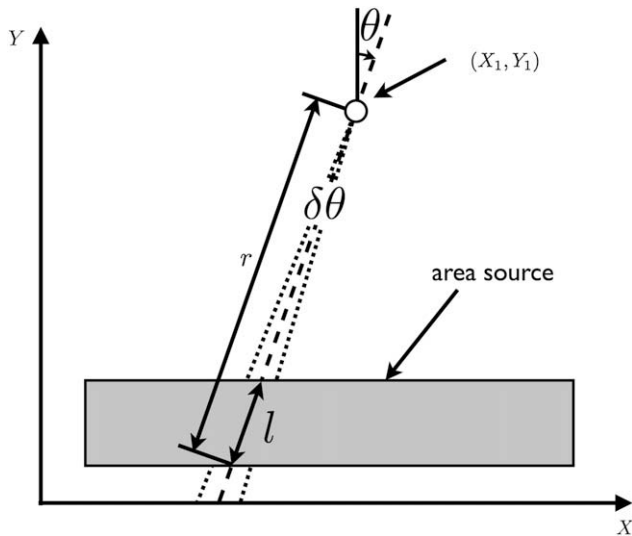


Fig. 3. Schematic of calculation of l and r for a particular receptor $(X, Y) = (X_1, Y_1)$ at angle θ . The polar nature of the coordinate system is indicated by $\delta\theta$, over which the integration is performed.

Note that $(r - x)$ cancels – i.e. the polar weighting balances the additional decay factor due to three-dimensional dispersion introduced by Receptor LDAA.

We define the impact of an angular area source slice under the Receptor LDAA approximation as

$$\chi_s(r, l) = \int_0^l \chi_v(x)(1 - r/x)dx, \tag{20}$$

which for many practical dispersion kernels can be analytically evaluated. Note that this is a solution for two-dimensional dispersion from an area source of length l . We have now reduced the five nested numerical integrals of Eq. (18) to two, i.e.

$$\langle \chi(X, Y) \rangle = \bar{q} \int \int I(\theta, \mathbf{m}) \chi_s(r, l) d\theta d\mathbf{m}. \tag{21}$$

In cases where the concentration on the area source is required, $l = r$ is taken as the distance from the upwind edge of the area source.

We compare the result of Eq. (21) to the ‘narrow plume assumption’, probably described first in an unpublished note by K.L. Calder and F.A. Gifford, 31 Dec. 1969, see Gifford and Hanna (1970); Calder (1976). The narrow plume assumption proposed that the two-dimensional dispersion kernel be used directly downwind of area sources, which is consistent with Eq. (21). It was derived rather differently; the key steps were to assume lateral dispersion according to a Dirac delta function and that emissions and meteorology are statistically independent. We have provided what can be interpreted as an alternative derivation of the narrow plume assumption, but allowing for correlation between meteorology and emissions, and accounting for lateral plume dispersion if the smoothed dispersion impact parameter is applied.

A conceptually similar approach was also described by Chitgopekar et al. (1990) for short-term dispersion from area sources. They used a probability density function $p(\theta)$ to represent wind direction fluctuations on a short time-scale, the direction in which χ_s acted varied according to this.

In the case where dispersion from ground-level sources is parameterized as per section 2.4, Eq. (20) can be analytically evaluated. Calculation of the annual mean concentration is thus given by

$$\langle \chi(X, Y) \rangle = \bar{q} \int \int I(\theta, \mathbf{m}) \frac{A}{1-s} [r^{1-s} - (r-l)^{1-s}] d\theta d\mathbf{m}. \tag{22}$$

A and s are evaluated at an effective value, e.g. at $x = l/2$.

4.3. Application of Source LDAA

We now invoke the approximation of sections 2.3.3 and 2.4 to develop an analytical solution for long-term three-dimensional dispersion from rectangular area sources. We begin with the finite line source solution developed in section 3.3 [Eq. (16)]. Taking the limit $1/w \rightarrow 0$ yields a solution for a semi-infinite line source:

$$\chi_l(X, Y) = \frac{A}{|X|^{s+1}} \left[Y {}_2F_1 \left(\frac{1-s+1}{2}, \frac{3}{2}; \frac{Y^2}{X^2} \right) - \frac{X \Gamma(\frac{s}{2}) \sqrt{\pi}}{2 \Gamma(\frac{s+1}{2})} \right]. \tag{23}$$

We then integrate this in X to obtain the indefinite integral

$$\chi_{A1}(X, Y) = \frac{A}{(1-s)^2 X^s} \left\{ \frac{X \Gamma(\frac{s}{2}) \sqrt{\pi}}{\Gamma(\frac{s-1}{2})} + Y(1-1/s) \times \left[{}_2F_1 \left(\frac{1-s+1}{2}, \frac{3}{2}; \frac{Y^2}{X^2} \right) - {}_2F_1 \left(\frac{s-s+1}{2}, \frac{s}{2} + 1; \frac{Y^2}{X^2} \right) \right] \right\}, \tag{24}$$

valid for $X > 0$. To see how the indefinite integral is used, consider the concentration at (X_0, Y_0) due to a semi-infinite ‘strip’ extending from the X -axis to infinite Y and from $X = 0$ to $X = l$ ($l < X_0$). The concentration at (X_0, Y_0) is given by the convolution of semi-infinite line sources, i.e.

$$\int_0^l \chi_l(X_0 - \tilde{X}, Y_0) d\tilde{X} = \chi_{A1}(X_0 - l, Y_0) - \chi_{A1}(X_0, Y_0),$$

which has been expressed in terms of Eq. (24).

In order to determine concentrations on the edge of the area source, a solution at $X = 0$ will be needed. The singularity at $X = 0$ in Eq. (24) is removable: taking the limit $X \rightarrow 0$ gives

$$\chi_{A0}(Y) = - \frac{Y^{1-s} \Gamma(s) \Gamma(\frac{s}{2} + 1) \sqrt{\pi}}{(1-s) \Gamma(\frac{s+1}{2}) \Gamma(s+1)}. \tag{25}$$

To simplify the description of the mathematics, we have considered only $X > 0$ and assumed the source and receptors are in quadrant I. The indefinite solutions on and away from the removable singularity are used to construct the required solution by

$$\chi_a(X, Y; w, L) = \begin{cases} [\chi_{A1}(X' - L, Y') - \chi_{A1}(X', Y')] - [\chi_{A1}(X' - L, Y' - w) - \chi_{A1}(X', Y' - w)], & X' > L, \\ [\chi_{A0}(Y') - \chi_{A1}(X', Y')] - [\chi_{A0}(Y' - w) - \chi_{A1}(X', Y' - w)], & X' = L, Y' = w, \\ \chi_a(Y, X; L, w), & Y' \geq w \\ [\chi_{A0}(Y') - \chi_{A1}(X', Y')] - [\chi_{A1}(w - Y', X') - \chi_{A1}(w - Y', X' - L)], & X' = L, \\ [\chi_{A0}(Y') - \chi_{A1}(X', Y')] + [\chi_{A0}(Y') - \chi_{A1}(L - X', Y')] & \\ - [\chi_{A1}(w - Y', X') - \chi_{A1}(w - Y', X' - L)], & X' > 0, \end{cases} \tag{26}$$

superposition. The long-term mean concentrations due to an area source centered on (0, 0), of length L along the X – axis and w along the Y – axis can be estimated using where $X' = |X| + L/2$ and $Y' = |Y| + w/2$ and the first case matched is taken.

We note a conceptual interpretation for the cases in Eq. (26). The first case corresponds to the receptor being to the east or west of the area source.⁴ Given the mapping to quadrant I, the indefinite solution for a semi-infinite area source can be most directly applied. The first term in square brackets corresponds to a semi-infinite area source starting from the X – axis. From this a second source shifted north by w is subtracted. In the second case, the receptor is on a corner, and χ_{A0} is used where the source meets the receptor. The third case corresponds to a receptor to the north or south of the area source. The basic solution [Eq. (24)] cannot be directly applied here, so we recursively evaluate χ_a with X and Y -related variables swapped. This then maps to the first case with variables swapped. The fourth case corresponds to receptors on the east or west area source edge, again χ_{A0} is applied to evaluate the upper limit of the integral and χ_{A1} the lower limit. Finally, the last case corresponds to a receptor on the area source. For this the area source is split into two, with analogies to the third case being applied for the portion to the east and west, but with coordinate directions and source geometrical parameters altered accordingly.

5. Results and discussion

5.1. Analytical solutions

We now present example analytical results for line and area sources. Evaluation of Gauss' hypergeometric function was based on the algorithm of Zhang and Jin (1996). Prototype implementation was in MATLAB 7.7 (The MathWorks, 2008). We take $A = 1$, $s = 0.8$ and $l = 1$ (i.e. isotropic meteorological conditions) on a 61×61 grid of receptors for these examples. Fig. 4 depicts long-term mean concentrations due to a line source as calculated by Eq. (16), and Fig. 5 shows an example result from the area source solution [Eq. (26)]. The computer runtimes for the line and area source algorithms were 1.7 and 5.0 s, respectively.

We now compare the new three-dimensional analytical line and area source solutions to the classical two-dimensional solutions for cross-wind line and area sources. Our motivation here is primarily validation.

As has been well established, given a two-dimensional cross-wind line source decay law of $\sim 1/X^s$ (as is compatible with the assumed functional form in the present paper), the corresponding short-term two-dimensional area source solution is of the form of the integrand in Eq. (22), e.g. Pasquill and Smith (1983) or Lebedefe and Hameed (1975) and K.L. Calder's comment on the article. Specifically, the concentration due to an infinite cross-wind area source extending from $X = 0$ to $X = l$ is given by

$$\chi(X) \propto \begin{cases} \int_0^l (X - \tilde{X})^{-s} d\tilde{X} \propto X^{1-s} - (X - l)^{1-s}, & X > l, \\ \int_0^X (X - \tilde{X})^{-s} d\tilde{X} \propto X^{1-s}, & 0 \leq X \leq l, \\ 0, & X < 0, \end{cases}$$

where the wind is from the negative X – direction. The interpretation is that upwind of the area source, zero concentrations are

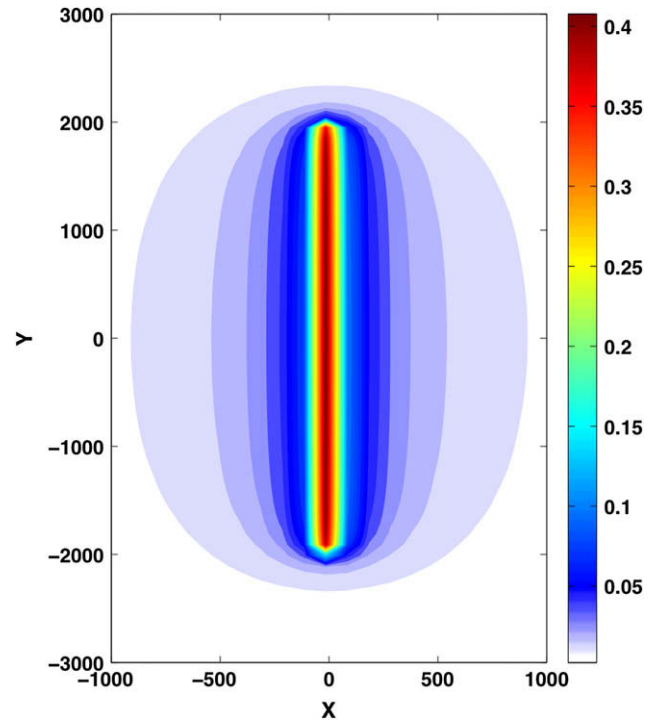


Fig. 4. Analytical solution for long-term mean dispersion from a line source of width $w = 4000$, with $l = A = 1$, $s = 0.8$ (arbitrary units).

assumed. Then on the area source concentrations grow as $\sim X^{1-s}$, before decaying rapidly after the area source by superposition of a shifted negative source.

In order to compare the well known two-dimensional solutions for short-term dispersion with our new three-dimensional solutions for long-term dispersion for line and area sources, we superpose two cases of the two-dimensional short-term solution: one where the wind is blowing in positive X – direction, and one in negative X – direction, with both cases centred on $X = 0$. The resulting solutions

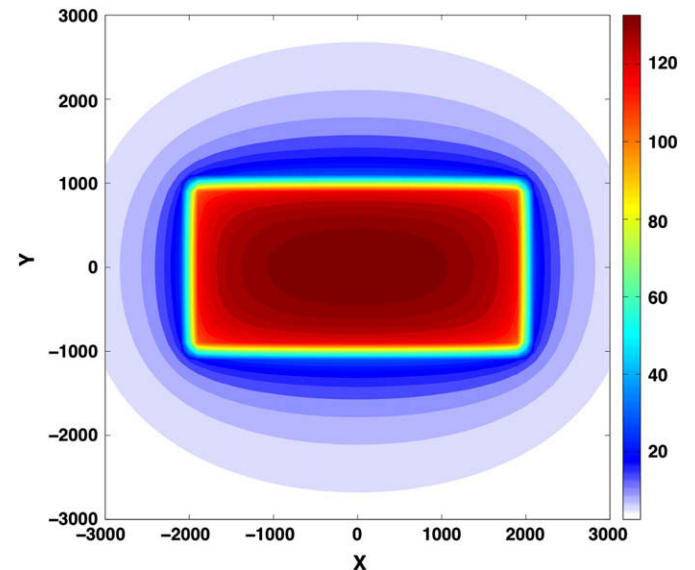


Fig. 5. Analytical solution for long-term mean dispersion from an area source of width $w = 2000$ and length $l = 4000$, with $l = A = 1$, $s = 0.8$ (arbitrary units).

⁴ For the purposes of this conceptual explanation 'north' corresponds to the positive Y – direction, not a geographic orientation.

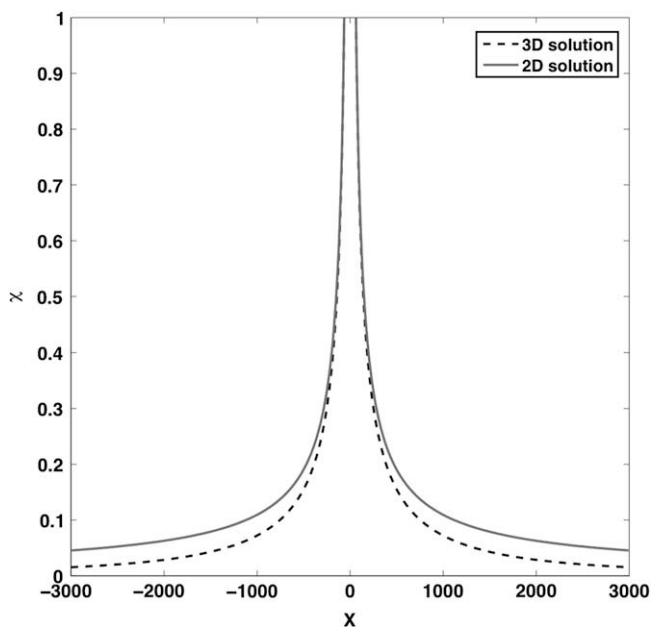


Fig. 6. Classic two-dimensional line source solution for wind blowing to the left and right summed and in comparison with the two-dimensional hypergeometric line source solution for a finite line source of length 4000 into the page (arbitrary units). Concentrations have been normalized.

are shown as the solid lines in Figs. 6 and 7, which correspond to line and area sources, respectively. The new long-term three-dimensional solutions are also shown.

The three-dimensional solution is based on equally likely wind directions, so the two-dimensional solution can be conceptualized as applying to the X – component of the wind direction. As would be expected, the three-dimensional concentration profile closely follows the two-dimensional solution though the centre of the area source (i.e. along $Y = 0$). While concentrations initially decay in a quasi-two-dimensional way near the source, the decay law for the three-dimensional solution must tend towards that of a point source. The more rapid decay of the three-dimensional solution away from the source is apparent in Figs. 6 and 7.

To numerically verify the long-term three-dimensional analytical area source solutions, a first order integration scheme for Eq. (22) was implemented, with integration being performed in an angular sense. Solutions were found to be identical to within numerical interpolation errors. The numerical integration approach [Eq. (22)] was three orders of magnitude slower than the analytical approach [Eq. (26)].

To explore the potential for efficiency gains from code optimization, the Gauss' hypergeometric function portion of the code was implemented in Fortran as a MATLAB shared library. This reduced area source execution time by a factor of 3.3. By applying compile-time optimization and implementing the algorithm implied by Eq. (26) in Fortran, execution time was improved a further 10-fold to 0.17 s.⁵

5.2. Example application

We now apply the methods developed to a simplified reference example of Heathrow Airport, London, UK to provide a first demonstration of the application of the methods. We consider NO_x emissions from aircraft on the ground at Heathrow Airport, UK. The total

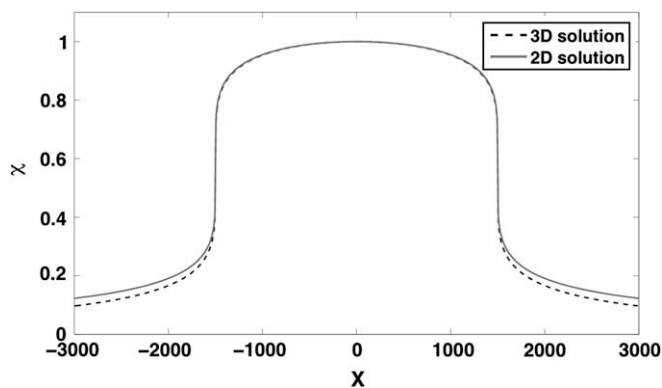


Fig. 7. Classic two-dimensional area source solutions for wind blowing to the left and right summed and in comparison with the two-dimensional hypergeometric area source solution for an area source of length 20,000 into the page and 3000 along the X – axis (arbitrary units). Concentrations have been normalized.

ground-level aircraft NO_x emissions for 2002 totaled 1768 tonnes, corresponding to a mean emission rate of $Q = 0.0561 \text{ kg}^{-1}$ (Underwood et al., 2004). The meteorological data used is also for 2002. We apportion all emissions to a single $2 \text{ km} \times 2 \text{ km}$ area source to facilitate comparison, and examine a $6 \text{ km} \times 6 \text{ km}$ domain with a receptor resolution of 100 m.

The analytical approach developed in this paper [Eq. (26)] was applied. A single AERMOD point source run was used to parameterize A and s with $\mathbf{T} = \{0, 10, \dots, 350\}^\circ$, and $\mathbf{R} = \{50, 100, 500, 1000, 5000, 10,000, 25,000\} \text{ m}$ (see section 2.4). A full time-series AERMOD area source calculation was also performed for 2002.

Results from the analytical approach and a full AERMOD calculation are shown in Fig. 8. The analytical approach took 3.8 s to execute and required a one-off 10 s AERMOD point source parameterization run. The full AERMOD area source calculation took 4.5 h.⁶ The rapid analytical approach yielded a 99.98% computation time saving for this case excluding the parameterization run.

The spatially averaged concentration differs by 0.8% between AERMOD and the rapid analytic approach (found from $\langle \chi_{\text{AERMOD}} \rangle / \langle \chi_{\text{Rapid}} \rangle$). The average error over all receptors is 5.8% (found from $\langle \chi_{\text{AERMOD}} / \chi_{\text{Rapid}} \rangle$). The first error metric is related to the overall accuracy of the method in a spatially averaged sense and the second metric indicates the degree of spatial accuracy.

The angular numerical integration scheme implemented for Eq. (22) was also used for the Heathrow example. This had an execution time of 1 h. The spatially averaged concentration differed from the analytic approach by 0.9% and the average error over all receptors by 2.7%, while being 950 times slower.

For comparison with BB08, we compare areas in exceedance of an arbitrarily chosen concentration of $\chi_r = 50 \mu\text{g m}^{-3}$. In BB08 we found that Receptor LDAA induces a +1.9% error in exceedance area. In this paper, the numerical integration scheme [Eq. (22)] relies upon Receptor LDAA and also the specified functional form [Eq. (10)]. An area bias of –0.9% was found. The analytical approach [Eq. (26)] relies upon Receptor and Source LDAA, the specified functional form, and the smoothing algorithm. The area error in this case was +1.1% at the $50 \mu\text{g m}^{-3}$ level. In the example application given, errors associated with new approximations are of a smaller magnitude than Receptor LDAA, which is the underpinning approximation.

⁵ The code was compiled and executed with the Intel Fortran Compiler 10.1.007 on a Mac OS X 10.5.6 computer with eight 2.8 GHz cores and 4 GB 667 MHz DDR2 RAM. A single core was used for execution.

⁶ AERMOD area source execution times are a function of source size. Execution times range from 20 min to 8 h for source dimensions on the scale of those considered in this paper.

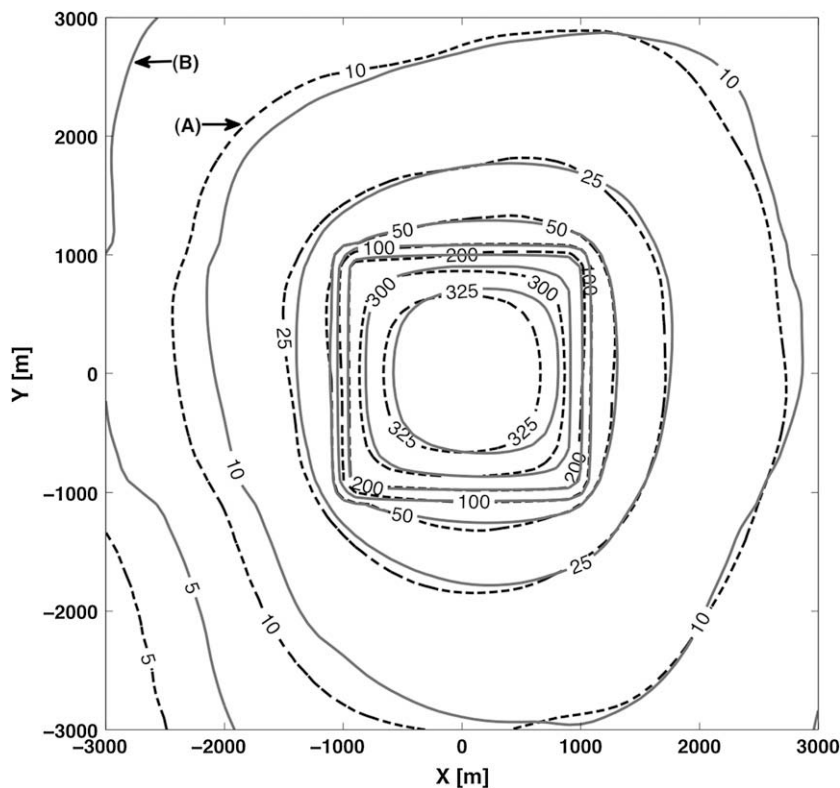


Fig. 8. London Heathrow example: NO_x concentrations [μgm^{-3}] due to a $2 \text{ km} \times 2 \text{ km}$ area source with a total emission rate of $0.0561 \text{ kg}(\text{NO}_x)\text{s}^{-1}$ as calculated by (A) the analytical area source solution [Eq. (26)] combined with Source LDAA, and parameterized by a point source AERMOD run, and (B) direct AERMOD calculation.

Additional information relating to the numerical errors associated with the rapid analytical methods can be found in the [Supplementary online material](#). In particular we note that:

- (i) the sign of the bias in exceedance area varies with the chosen threshold concentration, χ_r , and is generally less than 5% in magnitude; and
- (ii) the absolute error in concentration is less than $10 \mu\text{gm}^{-3}$ for over 95% of the modelling domain.

To put these error metrics in context, we compare to results of [UK Department for Transport \(2006\)](#), which evaluated the quality of several advanced dispersion models applied to Heathrow Airport. Model estimates of the land area in exceedance of the EU annual average NO_2 limit value of $40 \mu\text{gm}^{-3}$ varied by a factor of 1.6. This variation is attributable to differences in dispersion modelling, as a consistent emissions inventory was applied. As such, the additional errors introduced by the rapid analytical methods introduced here – typically less than 5% for an exceedance area – are small compared to modelling uncertainty.

6. Conclusions

The computational cost associated with the current generation of dispersion models can be prohibitive in the context of large-scale national or international policy assessments, where air quality predictions at thousands of sites may be required. We are working towards assessing the local air quality and health impacts of airports globally, which motivates our development of rapid modelling techniques for estimating long-term mean pollutant concentrations.

As the computational cost of current dispersion models is most acute for finite sources rather than point sources, and since line and area sources are most appropriate for representing runways, terminal

areas, roads, etc., we have focused on developing new mathematical and algorithmic techniques for their treatment. Analytical solutions were developed for estimating long-term mean dispersion from line and area sources under isotropic meteorological conditions. The solutions are based on Gauss' hypergeometric function, for which algorithms are well-developed. The isotropic assumption is then relaxed by parameterizing the solution with a single point source run using an existing advanced dispersion model.

In a Heathrow Airport example the rapid method parameterized by AERMOD resulted in a 5.8% average concentration error over all receptors (relative to direct AERMOD application), or an overall 0.8% error in spatially averaged pollutant concentration. These errors are an order of magnitude lower than dispersion modelling uncertainty. However, this may not hold in all applications or with all models. The analytical approach was 99.98% faster than a full AERMOD calculation. This level of computational efficiency gain may make possible wide-scale airport air quality analyses, as is the aim of the work. The approach is similarly suited to any dispersion application related to long-term average concentrations due to line and area sources, where errors on the order of a few percent compared to the parameterizing model are acceptable and/or where analyses are only possible given the 3–4 orders of magnitude computation saving afforded by this approach.

In future work we will further develop the analytical modelling techniques and examine applications to airports specifically, including the influence of aircraft plume dynamics on local dispersion and treatment of elevated releases.

Acknowledgements

The authors are grateful to UK Research Councils EPSRC and NERC for providing funding, and to colleagues in the Institute for Aviation and the Environment at Cambridge University for useful discussions.

Appendix A. Supplementary data

Supplementary data associated with this article can be found in the online version, at doi:[10.1016/j.atmosenv.2009.03.032](https://doi.org/10.1016/j.atmosenv.2009.03.032).

References

- Abramowitz, M., Stegun, I., 1964. Handbook of Mathematical Functions. In: Applied Mathematics Series, vol. 55. National Bureau of Standards.
- Barrett, S.R.H., Britter, R.E., 2008. Development of algorithms and approximations for rapid operational air quality modelling. *Atmospheric Environment* 42, 8105–8111.
- Britter, R.E., Hanna, S.R., Briggs, G.A., Robins, A., 2003. Short-range vertical dispersion from a ground level source in a turbulent boundary layer. *Atmospheric Environment* 37, 3885–3894.
- CERC, 2004. ADMS 3 User Guide. Cambridge Environmental Research Consultants Ltd., UK. version 3.2 Edition.
- Calder, K., 1952. Some recent British work on the problems of diffusion in the lower atmosphere. In: Proceedings of the US Tech. Conf. Air Pollution, vol. 787. McGraw–Hill, New York.
- Calder, K.L., 1973. On estimating air pollution concentrations from a highway in an oblique wind. *Atmospheric Environment* 7, 863–868.
- Calder, K.L., 1976. Multiple-source plume models of urban air pollution – their general structure. *Atmospheric Environment* 11, 403–414.
- Carruthers, D., Holroyd, R., Hunt, J.C.R., Weng, W., Robins, A., Apsley, D., Thomson, D., Smith, F., 1994. UK-ADMS: a new approach to modelling dispersion in the earth's atmospheric boundary layer. *Journal of Wind Engineering & Industrial Aerodynamics* 52, 139–153.
- Carruthers, D., Mckeown, A., Hall, D., Porter, S., 1999. Validation of ADMS against wind tunnel data of dispersion from chemical warehouse fires. *Atmospheric Environment* 33, 1937–1953.
- Chitgopekar, N.P., Reible, D.D., Thibodeaux, L.J., 1990. Modeling of short range air dispersion from area sources of non-buoyant toxics. *Journal of the Air & Waste Management Association* 40, 1121–1128.
- Cimorelli, A.J., Perry, S.G., Venkatram, A., Weil, J.C., Paine, R.J., Wilson, R.B., Lee, R.F., Petersand, W.D., Brode, R.W., Paumier, J.O., 2004. AERMOD: Description of Model Formulation (EPA-454/R-03-004). US Environmental Protection Agency, Office of Air Quality Planning and Standards, Emissions Monitoring and Analysis Division. Tech. rep.
- Esplin, G.J., 1995. Approximate explicit solution to the general line source problem. *Atmospheric Environment* 29, 1459–1463.
- Gifford, F.A., Hanna, S.R., 1970. Urban air pollution modelling, Paper No ME-320. In: Proceedings of 2nd International Clean Air Congress, Washington, D.C.
- Hanna, S.R., Egan, B.A., Purdum, J., Wagler, J., 2001. Evaluation of the ADMS, AERMOD, and ISC3 dispersion models with the OPTEX, Duke Forest, Kincaid, Indianapolis and Lovett field datasets. *International Journal of Environment and Pollution* 16 (1–6), 301–314.
- Hirtl, M., Baumann-Stanzer, K., 2007. Evaluation of two dispersion models (ADMS-Roads and LASAT) applied to street canyons in Stockholm, London and Berlin. *Atmospheric Environment* 41, 5959–5971.
- Janicke Consulting, 2009. <http://www.janicke.de>.
- Lebedefe, S.A., Hameed, S., 1975. Steady-state solution of the semi-empirical diffusion equation for area sources. *Journal of Applied Meteorology* 14, 546–549.
- Luhar, A.K., Patil, R.S., 1989. A general finite line source model for vehicular pollution prediction. *Atmospheric Environment* 23 (3), 555–562.
- Martin, D.O., 1971. An urban diffusion model for estimating long term average values of air quality. *Journal of the Air Pollution Control Association* 21 (1), 16–19.
- McHugh, C., Carruthers, D., Higson, H., Dyster, S., 2001. Comparison of model evaluation methodologies with application to ADMS 3 and US models. *International Journal of Environment and Pollution* 16 (1–6), 1–11.
- Nagendra, S., Khare, M., 2002. Line source emission modelling. *Atmospheric Environment* 36, 2083–2098.
- Pasquill, F., Smith, F.B., 1983. *Atmospheric Diffusion*. Ellis Horwood.
- Perry, S.G., Cimorelli, A.J., Paine, R.J., Brode, R.W., Weil, J.C., Venkatram, A., Wilson, R.B., Lee, R.F., Peters, W.D., 2005. AERMOD: a dispersion model for industrial source applications. Part II: model performance against 17 field study databases. *Journal of Applied Meteorology* 44 (5), 694–708.
- Reynolds, T.G., Barrett, S., Dray, L., Evans, A., Köhler, M., Schäfer, A., Vera Morales, M., Wadud, Z., Britter, R., Hallam, H., Hunsley, R., 2007. Modelling the Environmental & Economic Impacts of Aviation: introducing the aviation Integrated modelling Project. In: 7th AIAA aviation Technology, integration and operations Conference.
- The MathWorks, 2008. MATLAB 7.6.
- UK Department for Transport, 2006. Project for the Sustainable development of Heathrow: Report of the Airport Air Quality Technical Panels.
- UK Department for Transport, 2007. Adding Capacity at Heathrow – Consultation Summary Document. http://www.dft.gov.uk/consultations/open/heathrow_consultation/consultationdocument/.
- US EPA, 2000. User's guide for the assessment system for population exposure nationwide (ASPEN, version 1.1) model. US Environmental Protection Agency.
- Underwood, B.Y., Walker, C.T., Peirce, M.J., 2004. Heathrow emission inventory 2002: Part 1. Tech. Rep. netcen/AEAT/ENV/R/1657/Issue 4, netcen.
- Venkatram, A., Horst, T.W., 2006. Approximating dispersion from a finite line source. *Atmospheric Environment* 40, 2401–2408.
- Zhang, S., Jin, J., 1996. *Computation of Special Functions*. John Wiley & Sons, Inc., New York.